



Phosphonic acid modifiers for enhancing selective hydrodeoxygenation over Pt catalysts: The role of the catalyst support



Patrick D. Coan^a, Michael B. Griffin^b, Peter N. Ciesielski^c, J. Will Medlin^{a,*}

^a Department of Chemical and Biological Engineering, University of Colorado – Boulder, Boulder, CO 80309, United States

^b National Bioenergy Center, National Renewable Energy Laboratory, Golden, CO 80401, United States

^c Biosciences Center, National Renewable Energy Laboratory, Golden, CO 80401, United States

ARTICLE INFO

Article history:

Received 23 December 2018

Revised 22 February 2019

Accepted 10 March 2019

Keywords:

Platinum

Hydrodeoxygenation

Phosphonic acids

Self-assembled monolayers

ABSTRACT

Bifunctional catalysts comprised of both noble metal and Brønsted acid sites are of growing interest for many reactions, such as the hydrodeoxygenation (HDO) of oxygenates produced by the deconstruction of lignocellulosic biomass. One method of preparing a bifunctional metal-acid catalyst is to modify the **supporting material** of a metal catalyst with acid-containing ligands, such as phosphonic acids (PAs), which provide tunable Brønsted acid sites at the metal-support interface. Here, we explore the potential for PA modification to improve HDO rates on Al₂O₃, TiO₂, CeO₂, and SiO₂-Al₂O₃ supports. PAs containing either alkyl or carboxylic acid (CA) tails were used to modify Pt catalysts on each support. PA modification improved HDO rates for the model compound benzyl alcohol when applied to Pt supported by Al₂O₃, TiO₂, and CeO₂, but had a negative effect on the HDO rate of Pt/SiO₂-Al₂O₃. Measurements of the relative strength of Brønsted acid sites present on the modified and unmodified catalysts suggested that PAs improved HDO when they provided new or stronger Brønsted acid sites. Additionally, the strength of the Brønsted acid sites provided by PA modifiers were tunable by altering the tail functionality, which affected the rates of HDO. These results suggest that PAs can be used to modify a variety of supports to prepare bifunctional acid-metal catalysts.

© 2019 Elsevier Inc. All rights reserved.

1. Introduction

The development and understanding of multifunctional catalysts, which contain two or more distinct reactive sites, is an increasingly important area of heterogeneous catalysis research [1–4]. By incorporating different functionalities onto a single catalyst, complex reactions can be performed. These multifunctional catalysts can be used to accomplish cascade reactions over a single substrate or to improve the rate of a desirable reaction via cooperative interactions of the individual active sites [5–8]. One specific application for bifunctional heterogeneous catalysts is the upgrading of pyrolysis oil, produced from lignocellulosic biomass [9]. Pyrolysis oil is made up of thousands of components, the majority of which have a high oxygen content relative to traditional crude oil. Thus, a hydrodeoxygenation (HDO) step is required to upgrade pyrolysis oil to a mixture that is chemically similar to petroleum and compatible with existing refining technology [10]. Benzyl alcohol has been used as a probe compound for the lignin portion of pyrolysis oil [11,12]. Previous work has shown that the deoxygena-

tion of aromatic alcohols over Pt catalysts is highly competitive with dehydrogenation/decarbonylation steps and can be coverage dependent [13]. These competitive pathways for benzyl alcohol are shown in Fig. 1, where HDO of benzyl alcohol results in the formation of the desirable product toluene, while dehydrogenation and subsequent decarbonylation steps lead to the formation of benzaldehyde and benzene, respectively. Although oxygen can be removed during decarbonylation steps, direct C–O bond scission is preferred because it maximizes the carbon yields of bio-oil feedstocks.

Several studies have shown that efficient HDO of biomass-derived oxygenates occurs through a combination of hydrogenation and dehydration reactions, requiring a bifunctional catalyst that contains active sites for each step [10,14–16]. Noble metals (e.g. Pt, Pd) are known to be efficient hydrogenation catalysts as they readily activate H₂, while Brønsted acid sites are known to perform dehydration reactions [17,18]. Thus, an effective HDO catalyst may be prepared by combining noble metal and Brønsted acid sites. One method for preparing such a bifunctional catalyst is to modify the support with acid-containing ligands [19]. Previous work has shown that self-assembled monolayers (SAMs) deposited from phosphonic acid (PA) precursors can be applied to both

* Corresponding author.

E-mail address: medlin@colorado.edu (J.W. Medlin).

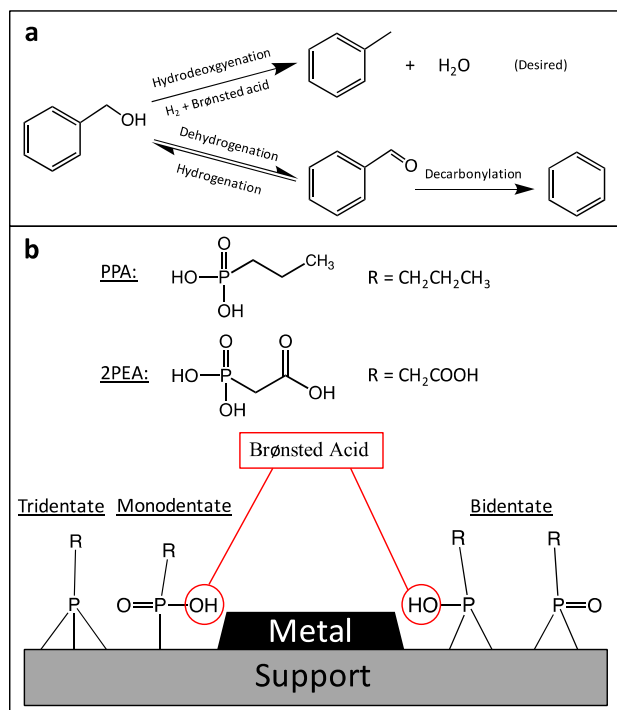


Fig. 1. (a) Reaction mechanism of benzyl alcohol over Pt catalysts, showing competitive hydrodeoxygenation and decarbonylation pathways (adapted from Ref. [21]). (b) Schematic representation of PA modifiers bound to supported metal catalysts, and structures of the modifiers propylphosphonic acid (PPA) and 2-phosphonopropionic acid (2PEA).

metal-oxide catalysts and the metal-oxide support of supported metal catalysts to influence reactivity [20–23]. PAs are known to bind to a variety of metal-oxides, forming up to three direct P–O–M (M = metal) bonds, and can provide Brønsted acid sites (P–OH) at the surface [24–30]. For supported noble metals, PAs have been used to modify Al_2O_3 -supported Pt and Pd catalysts and improve HDO in both the gas and liquid phases by incorporating Brønsted acidity at the metal-support interface [20–22]. It has been shown that the structure of the PA precursor can be adjusted to optimize the acid strength and HDO performance through inductive effects and intramolecular cooperativity [20,21]. As an additional benefit, PAs have also been found to improve the stability of metal-oxide supports in the harsh and acidic environments often encountered in pyrolysis oil upgrading [31]. Previous work has also analyzed the thermal stability of PA modifiers on a variety of metal-oxide surfaces, and found that the modifiers remain intact to temperatures at or above 400 °C in inert environments [20,21,31,32].

It is valuable to understand how changing the support can affect the enhancements observed by PA modification. Because PAs may interact differently with different supports [24–26], it is not known whether PAs will generally retain Brønsted acidity. As shown in Fig. 1, monodentate and possibly bidentate binding modes provide Brønsted acid sites on the catalyst support, while tridentate binding does not provide Brønsted acidity, but may provide surface crowding at the metal-support interface. It is also unclear whether the deposition of acid-containing PAs will improve HDO activity and selectivity relative to unmodified catalysts regardless of the support. In this study, we prepared four different supported Pt catalysts and deposited PAs containing either an alkyl or carboxylic acid (CA) tail to each (Fig. 1). These various supported catalysts exhibited differences in surface area, acid site strength, and metal dispersion; therefore, our main objective was to understand how application of PAs influenced properties and catalytic

behavior on diverse supported systems. Our previous work showed that the strength of Brønsted acid sites incorporated by PA modifiers is dependent on the tail functionality, with short-chain CA tails providing stronger acid sites than alkyl tails [20]. 2-Phosphonoethanoic acid (2PEA) was chosen as the phosphono-carboxylic acid (PCA) because it was found to provide the strongest Brønsted acid sites and the greatest enhancements in DO rates in our previous study [20]. Propylphosphonic acid (PPA) was chosen for comparison because it has a simple alkyl tail that is similar in size to 2PEA. The four supports (Al_2O_3 , TiO_2 , CeO_2 , $\text{SiO}_2\text{-Al}_2\text{O}_3$) were chosen so as to allow us to examine the effects of using reducible versus irreducible supports and the role of support acidity on the potential for PAs to improve HDO rates.

2. Experimental methods

2.1. Materials

The $\gamma\text{-Al}_2\text{O}_3$ (3 μm powder, 99.997% metals basis) and CeO_2 (15–30 nm APS powder, >99.5%) supports were purchased from Alfa Aesar. The TiO_2 support (P25, >99.5%) was purchased from Acros Organics. The $\text{SiO}_2\text{-Al}_2\text{O}_3$ support (GRACE Davicat® SIAL 3115, ~13 wt% Al_2O_3 , ~Si:Al = 5.7) was provided by W.R. Grace. 2-Phosphonoethanoic acid (98%), propylphosphonic acid (95%), benzyl alcohol (99.8%), and pyridine ($\geq 99\%$) were purchased from Sigma Aldrich. HPLC-grade tetrahydrofuran (>99.9%) was purchased from OmniSolv. Chloroplatinic acid hexahydrate ($\text{H}_2\text{PtCl}_6 \cdot 6\text{H}_2\text{O}$, 99.9%) was purchased from Strem Chemicals. All gases (Ultra-high purity H_2 , He, and Ar, 30% N_2/He , and 10% CO/He) were obtained from Airgas.

2.2. Catalyst preparation and characterization

Supported Pt catalysts were prepared by incipient wetness impregnation of Pt onto each support. Prior to catalyst synthesis, each support was dried in air at 120 °C for at least 12 h. Next, a solution of chloroplatinic acid hexahydrate ($\text{H}_2\text{PtCl}_6 \cdot 6\text{H}_2\text{O}$) in distilled water was prepared and mixed with the desired mass of support in order to achieve the desired Pt weight loading of approximately 3%. The resulting mixture was dried at 120 °C for 12 h to remove water, and the dried solid was then calcined in air at 400 °C for 4 h. Lastly, the calcined solid was reduced in 10% H_2/He at 250 °C for 2 h, resulting in the formation of metallic Pt nanoparticles.

BET surface area of each catalyst support was measured using a Micrometrics (Norcross, GA) Chemisorb 2720. Samples were pre-treated at 220 °C for 1 h in helium (20 sccm), then cooled to room temperature prior to nitrogen saturation with 30% nitrogen in helium. Adsorption and desorption of nitrogen were measured, and the desorption measurements were used to determine the powder surface area. Triplicate measurements were performed on each substrate, and the associated errors were propagated with errors from ICP-OES analysis to determine SAM surface density (Equations S7–S16). Samples were also analyzed with an ARL 3410+ inductively coupled optical emission spectrometer (ICP-OES) to measure elemental composition. A blank and three standards were used for calibration. Standards were made by diluting certified standards. The samples were dissolved using a modified technique developed by Farrell, Matthes and Mackie (1980) [33]. Briefly, this procedure starts by adding 5 ml of a 7:3 mixture of hydrochloric acid and hydrofluoric acid and then 2 ml of nitric acid to the digestion tubes, which are heated to 95 °C in a digestion block (HotBlock by Environmental Express) for approximately 2 h. Samples were then cooled and brought up to 50 ml with a 1.5 wt% boric acid solution. The samples were then reheated to

95 °C for approximately 15 min before being cooled to room temperature for analysis. Phosphonate coverages and the Pt weight loading were calculated from the data collected by this procedure, using the equations given in the Supporting Information (Equations S7–S16 for phosphonate coverages and Equations S17–S20 for Pt weight loadings).

Transmission electron microscopy (TEM) was performed on each of the uncoated catalysts to evaluate the particle size of the resulting Pt nanoparticles. Catalyst particles were suspended in ethanol at ~1% wt/vol. A volume of 7 μ l of the suspension was drop-cast onto 200 mesh, carbon-coated copper grids (SPI Supplies, West Chester, PA). Samples were air dried prior to imaging. Imaging was performed with a FEI Tecnai G2 20 Twin 200 kV LaB6 TEM (FEI, Hillsboro, OR) at an accelerating voltage of 200 kV. Images were captured with a Gatan UltraScan 1000 camera (Gatan, Pleasanton, CA). At least 20 images were obtained from at least 5 different particle clusters for each sample. Particle size analysis was performed manually using ImageJ software on a sample size of at least 100 particles. Representative images of each uncoated catalyst are provided in Fig. S1. The average Pt particle sizes on Pt/Al₂O₃, Pt/TiO₂, Pt/SiO₂-Al₂O₃, and Pt/CeO₂ were found to be 6.7 \pm 1.2 nm, 1.9 \pm 0.2 nm, 19.2 \pm 2.5 nm, and 4.0 \pm 1.9 nm, respectively, as reported in Table S1. As a complementary measure, the metal dispersion and Pt particle sizes of the uncoated catalysts were also measured by CO chemisorption on a Micrometrics (Norcross, GA) Chemisorb 2720. Samples were reduced in H₂ at 200 °C for 2 h, then cooled to room temperature prior to performing injections of 10% CO/He. For Pt/Al₂O₃, Pt/TiO₂, Pt/SiO₂-Al₂O₃, and Pt/CeO₂, the metal dispersion was found to be 58.0% \pm 1.7%, 55.1% \pm 3.2%, 2.4% \pm 0.2%, and 44.8% \pm 1.6%, respectively. These values and the corresponding estimated particle sizes are reported in Table S1.

Phosphonate SAMs were prepared on the synthesized catalysts (Pt/Al₂O₃, Pt/TiO₂, Pt/SiO₂-Al₂O₃, Pt/CeO₂) by a liquid deposition technique [23]. First, the mass of PA required for a full monolayer (assuming monodentate binding) on a desired mass of catalyst was determined by Equation S1, using reported values for the density of surface hydroxyl groups on each support [34–37]. Next, a 10 mM solution of PA in THF was prepared, containing a three-fold excess of PA relative to the number of moles required for a full monolayer. The desired mass of prepared catalyst powder was then added to the PA solution, and the resulting suspension was stirred for 12–16 h at ambient conditions. The solid was then separated by centrifugation in an Eppendorf 5804 centrifuge at 8000 rpm for 8 min and annealed at 120 °C for 6 h. The resulting solid was washed and centrifuged three times (at 8000 rpm for 8 min), using the same amount of THF used to prepare the initial solution, in order to remove any physisorbed PAs. Finally, the SAM coated powder was dried under vacuum at room temperature.

Powder X-ray diffraction (XRD) data were collected using a Rigaku Ultima IV diffractometer with a Cu K α source (40 kV, 44 mA). Diffraction patterns were collected in the 2 θ range of 20–80° at a scan rate of 4° min⁻¹. Samples (10–20 mg) were supported on a glass sample holder with a 0.2 mm recessed sample area and were pressed into the recession with a glass slide to obtain a uniform z-axis height. Data were compared to reference card files from the International Center for Diffraction Data (Pt: 00-001-1190, Rutile TiO₂: 00-001-1292, Anatase TiO₂: 00-001-0562, CeO₂: 00-002-1306, Al₂O₃: 00-004-0858) to confirm the identity and phase of the sample.

Infrared spectroscopy experiments were performed with 100 scans at 4 cm⁻¹ resolution using a Thermo Scientific Nicolet 6700 FT-IR. A closed cell attachment (Harrick) was used for diffuse reflectance infrared Fourier transform spectroscopy (DRIFTS). Spectra were collected in both the hydrocarbon stretching region and in the carbonyl stretching region, to verify the identity of alkyl

and CA acid tails, respectively. High temperature measurements were performed under 100 ml min⁻¹ Ar, by heating the sample to incremental temperatures and holding for 15 min, then cooling to 50 °C prior to collection of spectra. Background spectra of uncoated samples at 50 °C were subtracted to produce the reported spectra. Infrared spectroscopy analysis following pyridine adsorption was performed under a flow of 100 ml min⁻¹. All spectra were collected using 100 scans, and at a resolution of 4 cm⁻¹. Samples were first loaded into a closed cell attachment (Harrick) for DRIFTS and pretreated in He at 200 °C for at least 1 h. Samples were then cooled to 50 °C and a background spectra was collected. Pyridine was then dosed into the cell by flowing He through a pyridine bubbler, held at 0 °C, for 15 min. Next, the system was flushed in He for 1 h while holding at 50 °C prior to the collection of spectra. For higher temperature measurements, samples were heated to a desired temperature and held for 10 min, then cooled back to 50 °C for collection of spectra.

2.3. Reactor studies

Hydrogenation reactions were performed in a Pyrex tube, packed bed, continuous-flow reactor at atmospheric pressure. Helium was bubbled through a liquid reactant (benzyl alcohol) held in a heated water bath at 60 °C and mixed with H₂ and make-up He upstream of the reactor. The resulting feed stream had gas-phase mole fractions of Y_{H₂} = 15% and Y_{benzyl alcohol} = 0.075%, and a total gas flow rate of 83 sccm. Reactions were run at a temperature of 180 °C. The mass of each catalyst used was varied as needed to achieve a desired conversion. The feed stream and reactor effluent were analyzed using an SRI Instruments 8610C gas chromatograph equipped with a Restek MXT[®]-5 capillary column and a flame ionization detector. Each experiment was run to steady state, which was defined as running for at least 200 min and having a conversion within \pm 0.5% over 4 consecutive measurements, taken over a period of 1 h. Average conversion and selectivity were determined from these steady state measurements, and used with the number of active metal sites to calculate the reported turnover frequencies by Equations S2–S6. The number of metal active sites were determined by CO chemisorption of the unmodified catalysts. Because previous work has shown that PAs do not bind to the surface of supported or unsupported Pt nanoparticles, these values are not expected to change after surface modification, and were thus used to calculate turnover frequencies of the modified catalysts as well [21].

3. Results and discussion

3.1. Catalyst synthesis and characterization

Pt/Al₂O₃, Pt/TiO₂, Pt/SiO₂-Al₂O₃, and Pt/CeO₂ catalysts were modified with PPA and 2PEA. Thus, including the unmodified catalysts, a total of twelve catalysts were tested and compared in this study. Table 1 presents the total surface area of the unmodified catalysts and the Pt weight loading. Note that the BET surface area is reported for the unmodified catalyst support; previous work using γ -Al₂O₃ found that modification with PAs of similar size led to a decrease in BET surface area of approximately 25% [31]. We carried out DRIFTS experiments to confirm that catalysts were modified with the intended alkyl and carboxylic acid functionalities. DRIFT spectra of the modified catalysts were collected in the region of 2700–3000 cm⁻¹ to characterize the CH₃ and/or CH₂ stretching modes, shown in Fig. 2a. For catalysts modified with PPA, intense peaks were observed at approximately 2965 cm⁻¹ (asymmetric methyl stretching), 2910 cm⁻¹ (symmetric methyl stretching), 2934 cm⁻¹ (asymmetric methylene stretching) and 2880 cm⁻¹

Table 1
Catalyst support BET surface areas, Pt loadings, and densities of surface modifiers. Errors associated with BET surface area represent the standard deviation of three separate measurements on the starting support material prior to deposition of Pt. Pt loadings and densities of surface modifiers were determined by ICP-OES analysis, and the errors represent the standard deviation of three separate measurements.

Catalyst support	BET surface area (m ² g ⁻¹)	Pt wt%	PPA surface density (Phosphonates nm ⁻²)	2PEA surface density (Phosphonates nm ⁻²)
γ-Al ₂ O ₃	56 ± 3	3.1 ± 0.2	4.9 ± 0.8	5.0 ± 0.5
TiO ₂ (P25)	48 ± 5	2.7 ± 0.1	3.4 ± 0.6	3.5 ± 0.6
SiO ₂ -Al ₂ O ₃	354 ± 12	3.0 ± 0.1	2.2 ± 0.1	4.1 ± 0.2
CeO ₂	42 ± 4	2.8 ± 0.1	3.1 ± 0.4	3.3 ± 0.4

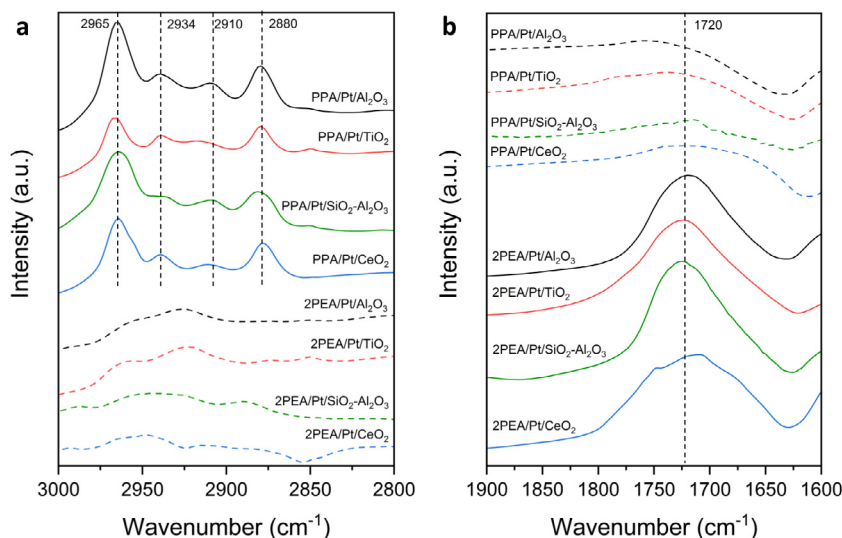


Fig. 2. FT-IR spectra of phosphonate coated Pt catalysts in (a) the hydrocarbon stretching region and (b) the carboxyl stretching region. Unmodified Pt catalysts for each support were used as the background for measurements of the coated catalysts. Spectra were scaled to improve visibility of relevant peaks.

(symmetric methylene stretching). The relatively high frequency of the asymmetric CH₂ stretching peak indicates considerable disorder in the monolayer, which is common for short-chain alkyl ligands [38]. Modification of catalysts using 2PEA resulted in a carboxylic acid-terminated monolayer, characterized by strong peaks in the region of 1700–1720 cm⁻¹ (C=O stretching) shown in Fig. 2b, indicating the presence of unbound CA tails. Asymmetric methylene stretching near 2960 cm⁻¹ was also observed in 2PEA-modified catalysts. Overall, both modifiers produced a somewhat disordered monolayer, as indicated by the higher frequencies of asymmetric CH₂ stretching, consistent with previous observations of monolayers having short chains and/or polar tails [28,38]. Furthermore, greater disorder has been shown to be consistent with under-coordinated binding of PAs, suggesting the presence of Brønsted acidity at the PA head group [28]. Spectra of the PPA-modified catalysts were also collected at high temperatures to verify the stability of these modifiers on each of the supports. Fig. S2 shows the spectra of each PPA-modified catalyst in the hydrocarbon stretching region at 50 °C and 400 °C. Comparison of these spectra suggests that the PA modifiers remain intact up to 400 °C, consistent with previous work [20,21,31,32].

XRD was performed to analyze the supporting materials both before and after PA modification. The results, shown in Fig. S3, confirmed the crystallinity of Al₂O₃ and CeO₂. The TiO₂ was determined to be mixed phase, as evidenced by a combination of diffractions from rutile and anatase crystallites. These results also show that deposition of PAs had no detectable effect on the bulk structure of the supporting materials. Additionally, previous work has suggested that PAs do not bind to the surface of Pt nanoparticles [21], and thus, the only apparent change to the prepared catalysts after PA deposition was the presence of PAs on the surface of the catalyst support.

ICP-OES analysis was used to determine the Pt wt% of the uncoated catalysts, as well as the density of PA modifiers on each coated catalyst, which are reported in Table 1. The measured Pt loadings exhibited good agreement with the nominal loading of 3 wt%. By detecting the relative amounts of phosphorus in each of the coated samples and using the measured BET surface areas of each support, the average density (in phosphonates nm⁻²) of 2PEA and PPA were determined on each catalyst. The highest coverages of approximately 5 phosphonates nm⁻² were observed on Pt/Al₂O₃. On Pt/TiO₂ and Pt/CeO₂, coverages of around 3 phosphonates nm⁻² were measured. Pt/SiO₂-Al₂O₃ was the only catalyst found to have significantly different coverages of the two modifiers; PPA had a coverage of only 2.2 phosphonates nm⁻², while 2PEA had a higher coverage of 4.1 phosphonates nm⁻². One possible explanation for the higher coverage of 2PEA on this support is that 2PEA contains stronger acid sites than PPA, which may lead to greater interaction with the strong Brønsted acid sites present on the SiO₂-Al₂O₃ support during deposition. However, further work is needed to identify the cause of this result.

3.2. Pyridine DRIFTS studies

Pyridine DRIFTS was used to characterize the acid sites on each of the twelve catalysts used in this study, shown in Fig. 3. Pyridine, when dosed onto acidic solid surfaces, exhibits characteristic stretching modes associated with Lewis and Brønsted acid sites [39,40]. Specifically, pyridine coordinately bound or hydrogen-bonded to Lewis acid sites exhibits stretching at ~1450 cm⁻¹ (1440 cm⁻¹–1460 cm⁻¹), whereas pyridinium ions adsorbed to Brønsted acid sites generally exhibit stretching at ~1540 cm⁻¹, but have been observed in the range of 1540–1550 cm⁻¹ [39,41–43]. Additionally, peaks near 1490 cm⁻¹ are observed, and

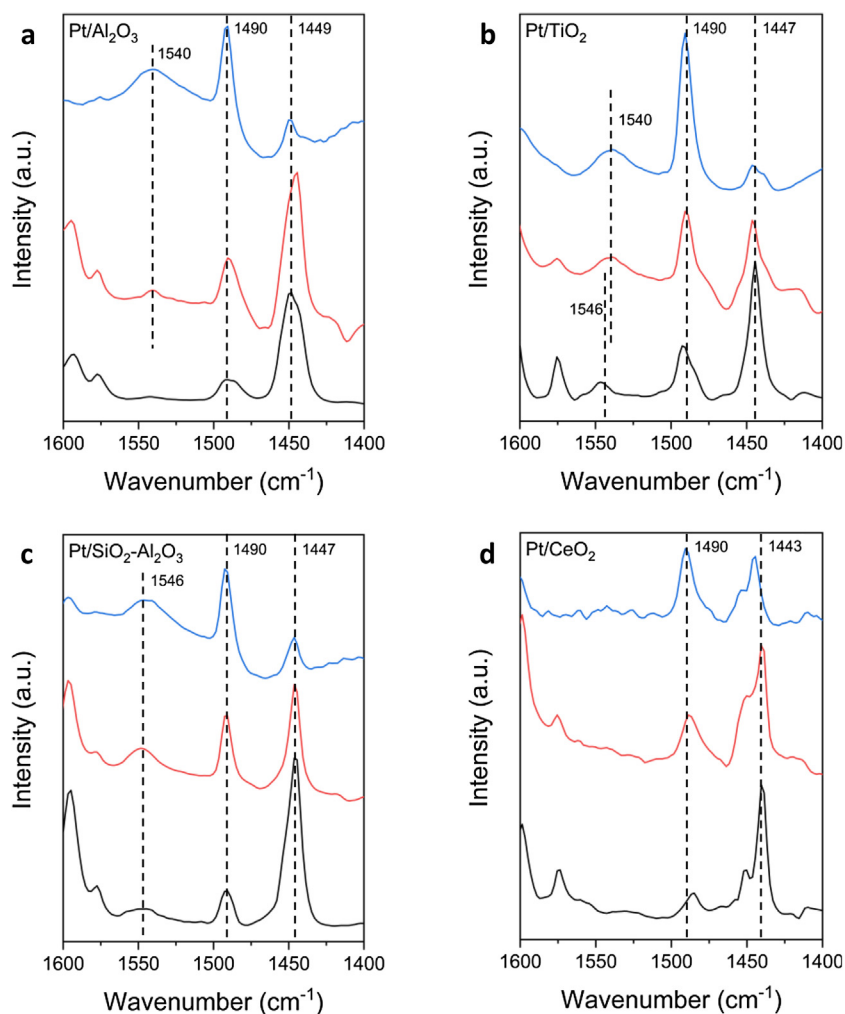


Fig. 3. FT-IR spectra of modified and unmodified (a) Pt/Al₂O₃ catalysts, (b) Pt/TiO₂ catalysts, (c) Pt/SiO₂-Al₂O₃ catalysts, and (d) Pt/CeO₂ catalysts, following pyridine dosing at 50 °C. Uncoated catalysts are shown in black (bottom), PPA coated catalysts are shown in red (middle), and 2PEA coated catalysts are shown in blue (top). Spectra prior to pyridine dosing were used as the backgrounds for all experiments. Spectra have been scaled as needed to improve visibility of relevant peaks.

represent a combination of both pyridine binding to Lewis acid sites (1488 cm⁻¹–1503 cm⁻¹) and pyridinium ion adsorption to Brønsted acid sites (1485 cm⁻¹–1500 cm⁻¹), although it has been suggested that this peak can be used to indicate Brønsted acidity [39]. Lewis acid sites on metal-oxides are associated with under-coordinated surface metal ions, and are expected to be present on all supports used here [44,45]. Brønsted acid sites are associated with surface hydroxyl groups that are partially positively charged, and thus able to protonate an adsorbed base [44,46].

On the Pt/Al₂O₃ catalysts, shown in Fig. 3a, both unmodified and modified catalysts exhibited Lewis acidity, as evidenced by the peaks near 1450 cm⁻¹ and 1490 cm⁻¹. On uncoated Pt/Al₂O₃, no Brønsted acidity was detected, as indicated by the lack of a clear peak at 1540 cm⁻¹. After PA modification, however, distinct peaks appeared around 1540 cm⁻¹, suggesting that both the PPA and 2PEA modifiers provided Brønsted acid sites at the catalyst surface. After modification with 2PEA, the appearance of the Brønsted acid peak (1540 cm⁻¹) was accompanied by a significant reduction in the Lewis acid peak (1450 cm⁻¹), and an increase in the peak at 1490 cm⁻¹, which represents binding to either Lewis or Brønsted acid sites [39,40]. Thus, modification of Pt/Al₂O₃ with 2PEA appeared to simultaneously increase Brønsted acidity and reduce the availability of Lewis acid sites on native γ -Al₂O₃. The Pt/TiO₂ catalysts, shown in Fig. 3b, exhibited a similar result, although a

small peak at 1546 cm⁻¹ was observed after dosing pyridine onto the uncoated catalyst, suggesting a small amount of Brønsted acidity [41,42]. After modification with PAs, this peak shifted to 1540 cm⁻¹, indicating a change in the nature of the Brønsted acid sites when PAs were present. Again, modification with 2PEA resulted in a significant reduction of the peak at 1450 cm⁻¹. On the Pt/SiO₂-Al₂O₃ catalysts, shown in Fig. 3c, Brønsted acidity was detected on the unmodified and PA-modified catalysts. This catalyst exhibited both Brønsted and Lewis acidity, as indicated by the peaks at 1540 cm⁻¹, 1490 cm⁻¹, and 1450 cm⁻¹. Modification with PAs did not alter the appearance of these three peaks. Additionally, modification with 2PEA again led to a reduction in the strength of the Lewis acid peak relative to the Brønsted acid peak.

Unexpectedly, there were no Brønsted acid peaks resolved around 1540 cm⁻¹ on any of the Pt/CeO₂ catalysts, as shown in Fig. 3d. Although the absence of Brønsted acidity on unmodified CeO₂ was expected, PA modification of the supports was expected to introduce Brønsted acid sites, similar to the Al₂O₃ support. The absence of a clearly resolvable peak near 1540 cm⁻¹ could indicate that PAs adsorb in a tridentate configuration in which acid sites are not introduced, or that any acid sites are simply weaker. One possible indication in support of the latter hypothesis is that on the PA-modified Pt/CeO₂ catalysts a significant increase in the peak

at 1490 cm^{-1} was observed. Because the peak at 1490 cm^{-1} is representative of pyridine binding to either Brønsted or Lewis acid sites, the increased intensity of this peak may suggest the presence of Brønsted acid sites after PA modification. The reactivity results presented below offer further support to this conjecture. Overall, the results of these experiments indicate the PA modifiers provide or increase the number of Brønsted acid sites to Pt/Al₂O₃ and Pt/TiO₂ catalysts, and possibly on Pt/CeO₂. Conversely, PA modification appears to have little to no effect on the presence of Brønsted acid sites on Pt/SiO₂-Al₂O₃.

Previous work has suggested that the strength of Brønsted acid sites present in bifunctional acid-metal catalysts can be correlated to the DO activity, with stronger acid sites providing the highest DO rates [20,21]. The relative strength of the Brønsted acid sites was therefore measured on uncoated and coated catalysts by observing the pyridinium desorption temperature with DRIFTS. In our previous study, this approach was used for Pd/Al₂O₃ catalysts modified with a variety of PAs, and it was found that short-chain PCAs, such as 2PEA, provided stronger acid sites compared to alkyl PAs, such as PPA [20]. A similar result would be expected for TiO₂ supported catalysts, because γ -Al₂O₃ and TiO₂ contain Lewis acid sites of similar strength [18]. Indeed, on the Pt/TiO₂ catalysts, it was found that the Brønsted acid strength followed the trend Pt/TiO₂ < PPA/Pt/TiO₂ < 2PEA/Pt/TiO₂. As shown in Fig. 4a, pyridine desorbed from Brønsted acid sites on Pt/TiO₂ at 240 °C, as indicated by the disappearance of the peak at 1544 cm^{-1} . On PPA/Pt/TiO₂, this peak persisted up to 260 °C, and up to 280 °C on 2PEA/Pt/TiO₂. Conversely, on the Pt/SiO₂-Al₂O₃ catalysts, the Brønsted acid sites present after PA modification were found to be weaker than those present on the unmodified catalyst. Instead, the Brønsted acid sites inherent to the SiO₂-Al₂O₃ support were found to be strongest, so that the acid strength trended as PPA/Pt/SiO₂-Al₂O₃ < 2PEA/Pt/SiO₂-Al₂O₃ < Pt/SiO₂-Al₂O₃. As shown in Fig. 4b, pyridine remained adsorbed to Brønsted acid sites on Pt/SiO₂-Al₂O₃ up to at least 500 °C, evidenced by the persistence of the peak at 1546 cm^{-1} . On 2PEA/Pt/SiO₂-Al₂O₃, this peak only persisted up to 300 °C, and to 200 °C on PPA/Pt/SiO₂-Al₂O₃. It is noted that pyridine desorption occurred below 400 °C on all PA-modified catalysts tested. Because it has been shown that PA modifiers remain intact on the surface up to temperature of at least 400 °C, it can be concluded that desorption of pyridine is dependent on the strength of adsorption to the acid sites provided by PA modifiers, and not due to the removal or decomposition of these sites [20,21,31,32].

On both the TiO₂ and SiO₂-Al₂O₃ supported catalysts, it was also found that PA modification weakened the strength of Lewis acid sites. This can be seen by observing the presence and relative size of the peak at or around 1450 cm^{-1} at increasing temperature. PA modifiers likely blocked Lewis acid sites on the support, lowering the signal even at low temperatures. Additionally, the peak around 1450 cm^{-1} was found to weaken significantly or even disappear at higher temperatures when PA modifiers were used. In general, by comparing the spectra of 2PEA- and PPA-modified catalysts, it appeared that 2PEA weakened the Lewis acid sites more so than PPA. One possible explanation for this difference is that the two modifiers have a different impact on the electronic structure of the support via through-surface inductive effects. However, previous computational work has indicated that changing the pendant organic ligands at positions remote from the P atom does not influence the local charges present on the support, even when strongly electron-withdrawing (e.g., -F) or -donating (-NH₂) groups are employed [23]. Another possible explanation is that the 2PEA modifier provides more steric hindrance or blocks Lewis acid sites through a direct carboxylic acid-surface interaction, reducing the availability of Lewis acid sites on the support. Finally, this difference may be due to a direct interaction between the CA tail of

2PEA with the surface, resulting in the weakening of nearby Lewis acid sites.

3.3. Hydrodeoxygenation of benzyl alcohol

Each catalyst was evaluated for the HDO of benzyl alcohol, with the goal being to determine how PA modification of each support affects the HDO performance relative to the uncoated catalysts. Catalysts were assessed at 5–15% steady state conversion of benzyl alcohol, except for the Pt/SiO₂-Al₂O₃ catalysts, which were assessed at less than 1% conversion. Due to the highly acidic nature of the SiO₂-Al₂O₃ support, higher conversions resulted in the formation of high molecular weight products, likely formed by condensation and coupling reactions, that quickly deactivated the catalysts at higher conversions. The overall rates, product formation rates, and product selectivities of each catalyst are summarized in Table S2. Control experiments were also performed using the unmodified catalyst supports, as well as each support modified with 2PEA. In these experiments, the only reactivity observed was low rates of dehydrogenation to form benzaldehyde (Fig. 1a). The rates of dehydrogenation (per mass of catalyst) accounted for less than 10% of the dehydrogenation rates observed when Pt was present, except on SiO₂-Al₂O₃, where the support was found to account for nearly 80% of the dehydrogenation activity.

When Al₂O₃ and TiO₂ supports were used, the effect of PA modification led to comparable changes in HDO performance. For both Pt/Al₂O₃ and Pt/TiO₂, modification with PPA led to a small decrease in the rate of production of toluene, the HDO product, as shown in Fig. 5. However, benzaldehyde production was found to decrease as well, so that the selectivity of toluene increased from 71% to 83% after PPA modification of Pt/Al₂O₃, and from 57% to 62% after modification of Pt/TiO₂, as shown in Fig. S4. When these catalysts were modified with 2PEA, which has been shown to provide stronger Brønsted acid sites than alkyl PAs [20], the rate of toluene production over Pt/Al₂O₃ increased by 1.5x, and by 1.9x over Pt/TiO₂. Additionally, the 2PEA-modified catalysts further increased the toluene selectivity to 92% over 2PEA/Pt/Al₂O₃ and 83% over 2PEA/Pt/TiO₂. The highest HDO rate of all catalysts studied here was measured over 2PEA/Pt/TiO₂, which was nearly double the rate measured over uncoated Pt/TiO₂. Consistent with previous observations, the catalysts containing stronger acid sites (Fig. 4) therefore yielded the higher rates of HDO.

In comparing the coated and uncoated catalysts, modification of Pt/CeO₂ yielded somewhat similar results to those found for the Pt/Al₂O₃ and Pt/TiO₂ catalysts, with the major difference being the effect of PPA. While this PA had little effect on the HDO performance of Pt/Al₂O₃ and Pt/TiO₂, it increased the rate of toluene production by a factor of 1.7 when deposited onto Pt/CeO₂. Modification with 2PEA further increased the rate of HDO, as expected, to nearly 2.3 times that of the uncoated catalyst. However, as opposed to uncoated Pt/Al₂O₃ and Pt/TiO₂, the rate of HDO measured over uncoated Pt/CeO₂ was quite low, and the toluene selectivity was only 6%, making it an undesirable catalyst for this reaction even after PA modification. Although the HDO rates increased after modification with PPA and 2PEA, the selectivity of toluene was only increased to 9% and 12%, respectively, as shown in Fig. S4. From the results of the TiO₂- and CeO₂-supported catalysts, which both showed increased rates of HDO after PA modification, it can be concluded that high reducibility of the support does not hinder the promotional effects of PAs. Although some previous reports have suggested that an oxygen-vacancy mechanism may be responsible for deoxygenation over reducible supports, the promotional effects observed here indicate that the PAs are still able to promote activity via a dehydration/hydrogenation mechanism [47,48].

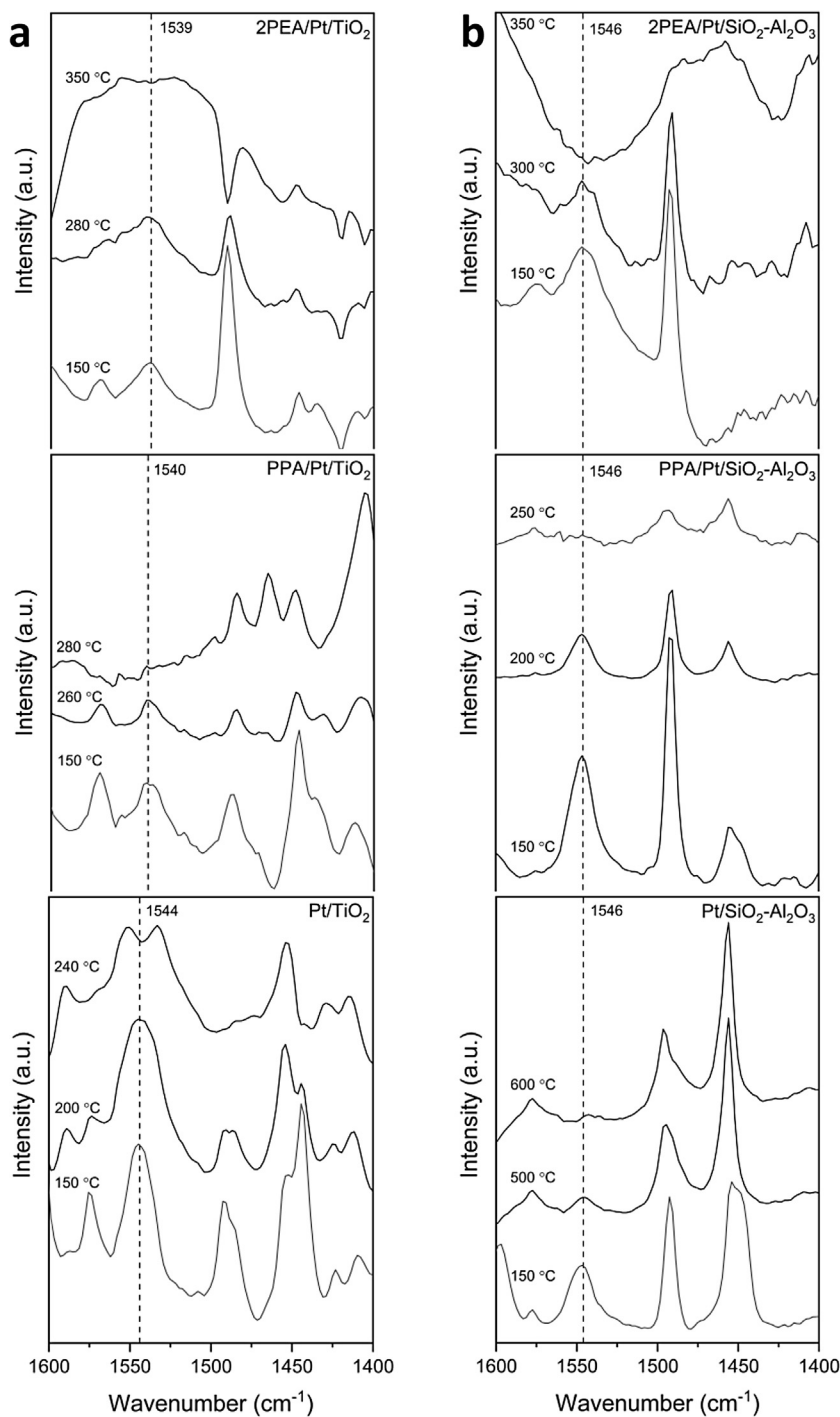


Fig. 4. Temperature-dependent pyridine DRIFTS spectra of coated and uncoated (a) Pt/TiO₂ catalysts and (b) Pt/SiO₂-Al₂O₃ catalysts. The Brønsted acid strengths of each catalyst were found to trend with the HDO activity.

Unlike the other three supports discussed above, PA modification of Pt/SiO₂-Al₂O₃ had a negative effect on HDO performance, regardless of the PA used. Uncoated Pt/SiO₂-Al₂O₃ was found to have a similar toluene production rate to that of uncoated Pt/Al₂O₃, and a toluene selectivity of 60%. After modification with PPA, the toluene production rate decreased by over 75%, and the toluene selectivity decreased to 48%. When 2PEA was used as the modifier, the toluene production rate was decreased by 68% compared to the uncoated catalyst, while the toluene selectivity improved to 67%. Although 2PEA/Pt/SiO₂-Al₂O₃ performed better overall than PPA/Pt/SiO₂-Al₂O₃, both catalysts performed signifi-

cantly worse for HDO than the unmodified catalyst. Moreover, modification of Pt/SiO₂-Al₂O₃ resulted in a substantial decrease in the overall activity of the catalyst, regardless of the modifier used, shown in Fig. S4.

Catalyst rates were also analyzed on the basis of interfacial area, assuming hemispherical particles. The results of this analysis are reported in Tables S3 and S4 for particle sizes measured by CO chemisorption and by TEM analysis, respectively. While this analysis does not affect the product selectivities or relative rates measured on a given catalyst before and after PA modification, it does affect the relative rates between the different supported catalysts,

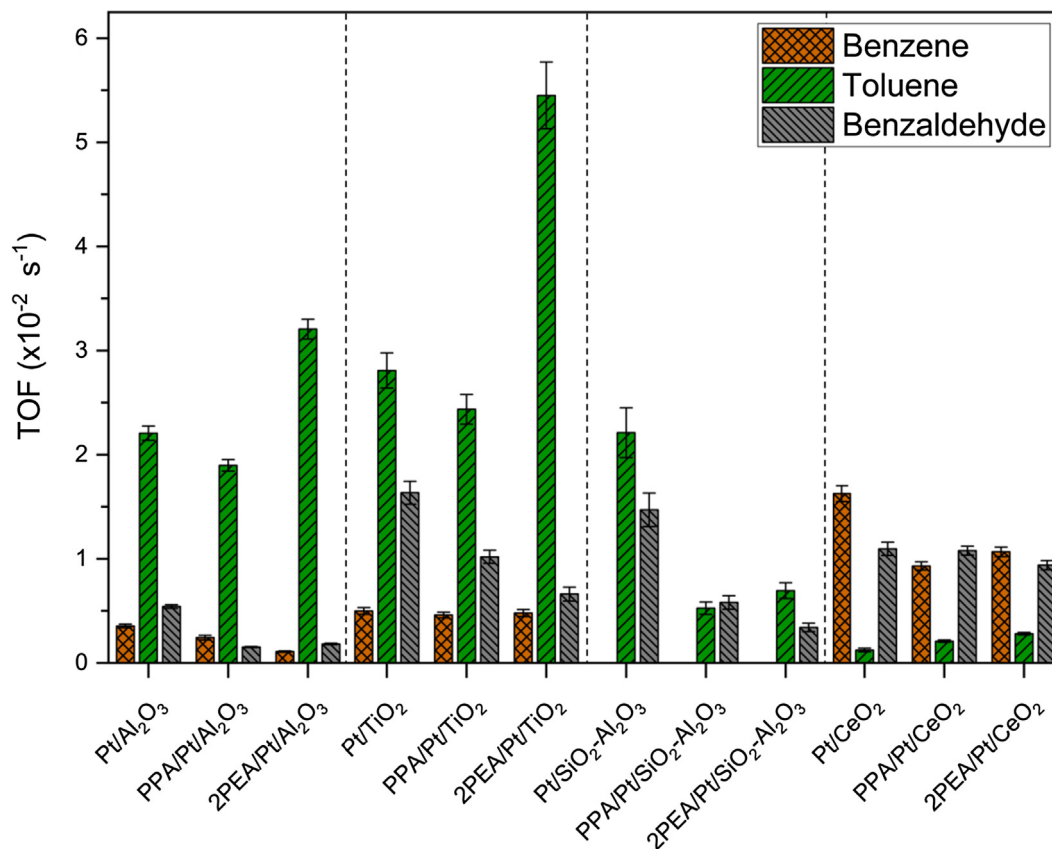


Fig. 5. Turnover frequencies (TOF) of products formed from benzyl alcohol under hydrogenation conditions. $T = 177\text{ }^{\circ}\text{C}$, $y_{\text{BA}} = 0.075\%$, $y_{\text{H}_2} = 15\%$, total flow of 83 sccm. The mass of catalyst was varied as needed to achieve a steady state conversion of $10 \pm 5\%$ for the Al_2O_3 , TiO_2 , and CeO_2 supported catalysts, and a steady state conversion of less than 1% for the $\text{SiO}_2\text{-Al}_2\text{O}_3$ supported catalysts. Error bars represent the standard deviation of three separate experiments.

due to the different particle sizes on each support. Turnover frequencies calculated on this basis caused the $\text{Pt}/\text{SiO}_2\text{-Al}_2\text{O}_3$ catalysts to increase relative to the other catalysts used in this study, due to the much larger Pt particle sizes measured on the $\text{SiO}_2\text{-Al}_2\text{O}_3$ support, particularly when particle sizes determined by CO chemisorption were used in the calculation. The use of interfacial area for rate normalization may be more appropriate for comparisons between the different supports used here, and are in better accordance with the expectation that $\text{SiO}_2\text{-Al}_2\text{O}_3$ supports should provide acid sites that are highly active for the deoxygenation reaction.

Overall, the results of these experiments suggest that PAs can improve HDO by one of two mechanisms. The first is to provide Brønsted acid sites at the metal-support interface of catalysts that do not have inherent Brønsted acidity, such as Al_2O_3 and possibly CeO_2 . The second is to provide stronger and more tunable acid sites to supports that may already have weak Brønsted acidity, such as TiO_2 . However, when a support with strong Brønsted acidity is used, such as $\text{SiO}_2\text{-Al}_2\text{O}_3$, PA modification only serves to replace or block these sites with potentially weaker sites, resulting in a loss of HDO activity. Thus, one way that different metal-oxide supports can result in different changes in HDO activity is that the Brønsted acid sites on the support can be different in character, and so the blocking or replacing of these sites by PAs has different effects on the HDO activity (either increasing or decreasing).

A further question that may arise is how the electronic structure of the metal-oxide support influences the strength of Brønsted acid sites in PA modifiers, and thus the extent of potential improvement on HDO activity due to modification. Because PAs bind directly to oxygen in the support, these atoms essentially serve as a ligand to the PA, and so the electronic structure of these atoms may influence the PA strength. One would expect a more negatively charged

surface oxygen atom to be associated with a more positively charged phosphorus atom, and consequently a stronger Brønsted acidity. We previously observed that pyridine desorbed from 2PEA-modified Al_2O_3 at $250\text{ }^{\circ}\text{C}$, whereas in this study pyridine remained adsorbed to 2PEA/ Pt/TiO_2 up to temperatures of $280\text{ }^{\circ}\text{C}$ (Fig. 4), indicating that PAs have stronger Brønsted acidity after deposition onto TiO_2 than Al_2O_3 . This is consistent with DFT calculations suggesting that the surface oxygen atoms present in TiO_2 carry a more negative charge those present in Al_2O_3 [49,50]. Furthermore, these results are consistent with the greater extent of increase in HDO activity observed after 2PEA-modification of Pt/TiO_2 compared to $\text{Pt}/\text{Al}_2\text{O}_3$ (Fig. 5). Thus, a second way that different metal-oxide supports can lead to different changes in HDO activity is that the electronic structure of the support may influence the Brønsted acid strength of the modifier, which in turn effects the degree of improvement in HDO.

While the electronic structure of the support can also influence the Lewis acidity, it is proposed that Lewis acid sites were not a major participant in HDO over the catalysts used in this study, as PA modification was found to weaken the Lewis acid sites, but generally improved HDO rates. Finally, the effect of PA modification to a mostly inert support, such as SiO_2 , may be of interest, though PAs were found to not deposit onto SiO_2 using the deposition procedure described herein.

4. Conclusion

PAs were used to modify the support surface of $\text{Pt}/\text{Al}_2\text{O}_3$, Pt/TiO_2 , $\text{Pt}/\text{SiO}_2\text{-Al}_2\text{O}_3$, and Pt/CeO_2 catalysts, and were tested in the HDO of benzyl alcohol. Over Al_2O_3 , TiO_2 , and CeO_2 -supported

catalysts, deposition of 2PEA was found to increase the rate of HDO, while deposition of PPA only improved the HDO rate when applied to Pt/CeO₂. When PAs were used to modify the support of Pt/SiO₂-Al₂O₃, which natively contains strong Brønsted acidity, the HDO performance was found to decrease by as much as 76%. Pyridine DRIFTS measurements suggested that improved rates of HDO were observed when modification with PAs led to incorporation of Brønsted acid sites or provided stronger Brønsted acid sites than those present prior to modification. Additionally, all catalysts modified with 2PEA, which is known to provide stronger acid sites than PPA, performed better than the equivalent catalyst modified with PPA. Overall, the results reported here show that PAs can be deposited onto a variety of catalyst supports and can provide substantial enhancements in HDO rates and selectivity, with the exception of a supporting material that already contains an abundance of strong acid sites. More broadly, these results suggest that PAs can be used to modify a variety of metal oxide supports, and are capable of strongly influencing catalyst reactivity, opening the door to a wide variety of materials and chemistries that can be examined using PA modification.

Acknowledgements

This work was funded by the US Department of Energy, Office of Science, Basic Energy Sciences Program, Chemical Sciences, Geosciences and the Biosciences Division, under Grant No. DE-SC0005239. Additional support for sample characterization was provided by the U.S. Department of Energy, Office of Energy Efficiency and Renewable Energy (EERE), Bioenergy Technologies Office (BETO), under Contract DE-AC36-08-GO28308 at the National Renewable Energy Laboratory (NREL). The research was performed in collaboration with the Chemical Catalysis for Bioenergy Consortium (ChemCatBio), a member of the Energy Materials Network (EMN). The views expressed in this article do not necessarily represent the views of the U. S. Department of Energy or the United States Government. P.D.C. acknowledges partial support from the Department of Education Graduate Assistantship in Areas of National Need (GAANN). The authors gratefully acknowledge Dr. Fred Luiszer for performing ICP-OES analysis. P.D.C. also wishes to thank Dr. Jing Zhang and Dr. Pengxiao Hao for useful discussions.

Appendix A. Supplementary material

Supplementary data to this article can be found online at <https://doi.org/10.1016/j.jcat.2019.03.011>.

References

- [1] G.W. Huber, J.N. Chheda, C.J. Barrett, J.A. Dumesic, Production of liquid alkanes by aqueous-phase processing of biomass-derived carbohydrates, *Science* 308 (5727) (2005) 1446–1450.
- [2] M.B. Griffin, G.A. Ferguson, D.A. Ruddy, M.J. Bidy, G.T. Beckham, J.A. Schaidle, Role of the support and reaction conditions on the vapor-phase deoxygenation of *m*-cresol over Pt/C and Pt/TiO₂ catalysts, *ACS Catal.* 6 (4) (2016) 2715–2727.
- [3] J.C. Serrano-Ruiz, J.A. Dumesic, Catalytic routes for the conversion of biomass into liquid hydrocarbon transportation fuels, *Energy Environ. Sci.* 4 (1) (2011) 83–99.
- [4] J.N. Chheda, G.W. Huber, J.A. Dumesic, Liquid-phase catalytic processing of biomass-derived oxygenated hydrocarbons to fuels and chemicals, *Angew. Chem. Int. Ed.* 46 (2007) 7164–7183.
- [5] R.K. Zeidan, S.J. Hwang, M.E. Davis, Multifunctional heterogeneous catalysts: SBA-15-containing primary amines and sulfonic acids, *Angew. Chem. Int. Ed.* 45 (2006) 6332–6335.
- [6] R.K. Zeidan, M.E. Davis, The effect of acid-base pairing on catalysis: an efficient acid-base functionalized catalyst for aldol condensation, *J. Catal.* 247 (2007) 379–382.
- [7] E.L. Margelefsky, R.K. Zeidan, M.E. Davis, Cooperative catalysis by silica-supported organic functional groups, *Chem. Soc. Rev.* 37 (2008) 1118–1126.
- [8] J.M. Notestein, A. Katz, Enhancing heterogeneous catalysis through cooperative hybrid organic-inorganic interfaces, *Chem. Eur. J.* 12 (2006) 3954–3965.
- [9] P.N. Ciesielski, M.B. Pecha, V.S. Bharadwaj, C. Mukarakate, G.J. Leong, B. Kappes, M.F. Crowley, S. Kim, T.D. Foust, M.R. Nimlos, Advancing catalytic fast pyrolysis through integrated multiscale modeling and experimentation: challenges, progress, and perspectives, *WIREs Energy Environ.* 7 (4) (2018) 1–19.
- [10] D.A. Ruddy, J.A. Schaidle, J.R. Ferrell III, J. Wang, L. Moens, J.E. Hensley, Recent advances in heterogeneous catalysts for bio-oil upgrading via “ex Situ Catalytic Fast Pyrolysis”: catalyst development through the study of model compounds, *Green Chem.* 16 (2014) 454–490.
- [11] K.L. Deutsch, B.H. Shanks, Hydrodeoxygenation of Lignin Model Compounds over a Copper Chromite Catalyst, *Appl. Catal. A* 447–448 (2012) 144–150.
- [12] A.M. Robinson, J.E. Hensley, J.W. Medlin, Bifunctional catalysts for upgrading of biomass-derived oxygenates: a review, *ACS Catal.* 6 (8) (2016) 5026–5043.
- [13] L.O. Mark, A.H. Jenkins, H. Heinz, J.W. Medlin, Furfuryl alcohol deoxygenation, decarbonylation, and ring-opening on Pt (111), *Surf. Sci.* 677 (2018) 333–340.
- [14] R.C. Nelson, B. Baek, P. Ruiz, B. Goundie, A. Brooks, M.C. Wheeler, B.G. Frederick, L.C. Grabow, R.N. Austin, Experimental and theoretical insights into the hydrogen-efficient direct hydrodeoxygenation mechanism of phenol over Ru/TiO₂, *ACS Catal.* 5 (11) (2015) 6509–6523.
- [15] D.D. Laskar, B. Yang, H. Wang, J. Lee, Pathways for biomass-derived lignin to hydrocarbon fuels, *Biofuels Bioprod. Bioref.* 7 (2013) 602–626.
- [16] M. Besson, P. Gallezot, C. Pinel, Conversion of biomass into chemicals over metal catalysts, *Chem. Rev.* 114 (2014) 1827–1870.
- [17] G.W. Huber, R.D. Cortright, J.A. Dumesic, Renewable alkanes by aqueous-phase reforming of biomass-derived oxygenates, *Angew. Chem. Int. Ed.* 43 (12) (2004) 1549–1551.
- [18] A. Corma, Inorganic solid acids and their use in acid-catalyzed hydrocarbon reactions, *Chem. Rev.* 95 (3) (1995) 559–614.
- [19] N.C. Nelson, Z. Wang, P. Naik, J.S. Manzano, M. Pruski, I.I. Slowing, Phosphate modified ceria as a Brønsted acidic/redox multifunctional catalyst, *J. Mater. Chem. A* 5 (2017) 4455–4466.
- [20] P.D. Coan, L.D. Ellis, M.B. Griffin, D.K. Schwartz, J.W. Medlin, Enhancing cooperativity in bifunctional acid – Pd catalysts with carboxylic acid-functionalized organic monolayers, *J. Phys. Chem. C* 122 (2018) 6637–6647.
- [21] J. Zhang, L.D. Ellis, B. Wang, M.J. Dzara, C. Sievers, S. Pylypenko, E. Nikolla, J.W. Medlin, Control of interfacial acid-metal catalysis with organic monolayers, *Nat. Catal.* 1 (2018) 148–155.
- [22] P. Hao, D.K. Schwartz, J.W. Medlin, Phosphonic acid promotion of supported Pd catalysts for low temperature vanillin hydrodeoxygenation in ethanol, *Appl. Catal. A* 561 (2018) 1–6.
- [23] L.D. Ellis, R.M. Trotter, C.B. Musgrave, D.K. Schwartz, J.W. Medlin, Controlling the surface reactivity of titania via electronic tuning of self-assembled monolayers, *ACS Catal.* 7 (2017) 8351–8357.
- [24] S. Pawsey, K. Yach, L. Reven, Self-assembly of carboxyalkylphosphonic acids on metal oxide powders, *Langmuir* 18 (13) (2002) 5205–5212.
- [25] T. Bauer, T. Schmaltz, T. Lenz, M. Halik, B. Meyer, T. Clark, Phosphonate- and carboxylate-based self-assembled monolayers for organic devices: a theoretical study of surface binding on aluminum oxide with experimental support, *ACS Appl. Mater. Interfaces* 5 (13) (2013) 6073–6080.
- [26] R. Lushtinetz, G. Seifert, E. Jaehne, H.J.P. Adler, Infrared spectra of alkylphosphonic acid bound to aluminium surfaces, *Macromol. Symp.* 254 (2007) 248–253.
- [27] R. Lushtinetz, A.F. Oliveira, J. Frenzel, J.O. Joswig, G. Seifert, H.A. Duarte, Adsorption of phosphonic and ethylphosphonic acid on aluminum oxide surfaces, *Surf. Sci.* 602 (7) (2008) 1347–1359.
- [28] R. Lushtinetz, A.F. Oliveira, H.A. Duarte, G. Seifert, Self-assembled monolayers of alkylphosphonic acids on aluminum oxide surfaces—a theoretical study, *Z. Anorg. Allg. Chem.* 636 (8) (2010) 1506–1512.
- [29] H. Dietrich, T. Schmaltz, M. Halik, D. Zahn, Molecular dynamics simulations of phosphonic acid-aluminum oxide self-organization and their evolution into ordered monolayers, *Phys. Chem. Chem. Phys.* 19 (2017) 5137–5144.
- [30] M. Nilsing, S. Lunell, P. Persson, L. Ojamäe, Phosphonic acid adsorption at the TiO₂ anatase (101) surface investigated by periodic hybrid HF-DFT computations, *Surf. Sci.* 582 (1–3) (2005) 49–60.
- [31] T.V. Cleve, D. Underhill, M.V. Rodrigues, C. Sievers, J.W. Medlin, Enhanced hydrothermal stability of γ-Al₂O₃ catalyst supports with alkyl phosphonate coatings, *Langmuir* 34 (2018) 3619–3625.
- [32] L.D. Ellis, J. Ballesteros-Soberanas, D.K. Schwartz, J.W. Medlin, Effects of metal oxide surface doping with phosphonic acid monolayers on alcohol dehydration activity and selectivity, *Appl. Catal. A* (2018).
- [33] R.F. Farrell, S.A. Matthes, A.J. Mackie, Simple low-cost method for the dissolution of metal and mineral samples in plastic pressure vessels, *Rep. Investig. – Bur. Mines* (1980) 8480.
- [34] M. Digne, P. Sautet, P. Raybaud, P. Euzen, H. Toulhoat, Use of DFT to achieve a rational understanding of acid–basic properties of γ-alumina surfaces, *J. Catal.* 226 (2004) 54–68.
- [35] R. Mueller, H.K. Kammler, K. Wegner, S.E. Pratsinis, OH surface density of SiO₂ and TiO₂ by thermogravimetric analysis, *Langmuir* 19 (1) (2003) 160–165.
- [36] H. Yuan, D. Guo, X. Li, L. Yuan, W. Zhu, L. Chen, X. Qiu, The effect of CeO₂ on Pt/CeO₂/CNT catalyst for CO electrooxidation, *Fuel Cells* 9 (2) (2009) 121–127.
- [37] J.G. Larson, W.K. Hall, Studies of the hydrogen held by solids. VII. The exchange of the hydroxyl groups of alumina and silica-alumina catalysts with deuterated methane, *J. Phys. Chem.* 69 (9) (1965) 3080–3089.
- [38] A. Ulman, Formation and structure of self-assembled monolayers, *Chem. Rev.* 96 (1996) 1533–1554.

- [39] E.P. Parry, An infrared study of pyridine adsorbed on acidic solids. Characterization of surface acidity, *J. Catal.* 2 (5) (1963) 371–379.
- [40] C.A. Emeis, Determination of integrated molar extinction coefficients for infrared absorption bands of pyridine adsorbed on solid acid catalysts, *J. Catal.* 141 (2) (1993) 347–354.
- [41] C.R. Reddy, Y.S. Bhat, G. Nagendrappa, B.S.J. Prakash, Brønsted and Lewis acidity of modified montmorillonite clay catalysts determined by FT-IR spectroscopy, *Catal. Today* 141 (2009) 157–160.
- [42] B. Chakraborty, B. Viswanathan, Surface acidity of MCM-41 by in situ IR studies of pyridine adsorption, *Catal. Today* 49 (1999) 253–260.
- [43] A. Platon, W.J. Thomson, Quantitative Lewis/Brønsted ratios using DRIFTS, *Ind. Eng. Chem. Res.* 42 (2003) 5988–5992.
- [44] M.I. Zaki, M.A. Hasan, L. Pasupulety, Surface reactions of acetone on Al_2O_3 , TiO_2 , ZrO_2 , and CeO_2 : IR spectroscopic assessment of impacts of the surface acid-base properties, *Langmuir* 17 (2001) 768–774.
- [45] A.L. Farragher, Surface vacancies in close packed crystal structures, *Adv. Colloid Interface Sci.* 11 (1979) 3–41.
- [46] M.I. Zaki, H. Knözinger, Carbon monoxide – a low temperature infrared probe for the characterization of hydroxyl group properties on metal oxide surfaces, *Mater. Chem. Phys.* 17 (1987) 201–215.
- [47] P.M. de Souza, R.C. Rabelo-Neto, L.E.P. Borges, G. Jacobs, B.H. Davis, D.E. Resasco, F.B. Noronha, Hydrodeoxygenation of phenol over Pd catalysts. Effect of support on reaction mechanism and catalyst deactivation, *ACS Catal.* 7 (3) (2017) 2058–2073.
- [48] S.M. Schimming, O.D. LaMont, M. König, A.K. Rogers, A.D. D'Amico, M.M. Yung, C. Sievers, Hydrodeoxygenation of guaiacol over Ceria – Zirconia catalysts, *ChemSusChem* 8 (2015) 2073–2083.
- [49] F. Labat, P. Baranek, C. Adamo, Structural and electronic properties of selected rutile and anatase TiO_2 surfaces: an Ab initio investigation, *J. Chem. Theory Comput.* 4 (2008) 341–352.
- [50] H.A. Dabbagh, M. Zamani, B.H. Davis, Nanoscale surface study and reactions mechanism of 2-butanol over the γ -alumina (100) surface and nanochannel: a DFT study, *J. Mol. Catal. A Chem.* 333 (2010) 54–68.